CLM-P60

United Kingdom Atomic Energy Authority

RESEARCH GROUP

Preprint

GAS LASER DETERMINATION OF THE ELECTRON DENSITY IN THE AFTERGLOW OF A HYDROGEN DISCHARGE

J. M. P. QUINN

Culham Laboratory,

Culham, Abingdon, Berkshire

1964

UNCLASSIFIED
(Approved for publication)

CLM - P 60

GAS LASER DETERMINATION OF THE ELECTRON DENSITY IN THE AFTERGLOW OF A HYDROGEN DISCHARGE

by

J.M.P. QUINN
(Submitted for publication in J. Nucl. Energy Pt C)

A B S T R A C T

A helium-neon gas laser interferometer has been used to investigate the electron density variation, both spatial and temporal, in the afterglow of a z-pinch in hydrogen at 100 mTorr. The percentage ionization, defined as the rate of the electron density to the initial gas density, was shown to drop from 100% to 1% in two phases. During the first phase, lasting 10 μsec, the dominating process was recombination. In the second phase lasting a further 90 μsec, ambipolar diffusion took over completely. Also, the results obtained for the density variation on the axis are compared with similar determinations using completely independent techniques.

U.K.A.E.A. Research Group,
Culham Laboratory,
Nr. Abingdon,
Berks.

September 1964 (C18/ED)

C O N T E N T S

1. INTRODUCTION

A helium-neon gas laser interferometer, as described by ASHBY and JEPHCOTT (1963), has been used to investigate the electron density variation, both spatial and temporal, in the afterglow of a z-pinch in hydrogen at 100 millitorr. This discharge is used as a preionization discharge for a megajoule θ-pinch experiment where it is essential, when comparing theory and experiment, to know the initial plasma conditions as closely as possible. The percentage ionization, defined as the ratio of the electron density to the initial gas density, was shown to drop from 100% to 1% in two phases. During the first phase, lasting 10 μsec, the dominating process was recombination. In the second phase, lasting a further 90 μsec, ambipolar diffusion took over completely. Further, the results obtained for the density variation on the axis are compared with similar determinations using completely independent techniques.

2. THE INTERFEROMETER

The interferometer consists of a helium-neon gas laser with an external mirror, placed so that it reflects light back into the laser cavity (see Fig.1). The laser cavity is that between mirrors M_1 and M_2, the external cavity is that between mirrors M_2 and M_3. Interference takes place, within the laser cavity, between the light reflected by M_2 and that from M_3. The light reflected by M_3 has a phase, at M_2, which controls the feedback in the laser cavity and hence its output intensity. Changes in the optical path length between M_2 and M_3 thus change the laser intensity.

The helium-neon laser emits two lines, at 0.63 μ and 3.39 μ, with a common upper level. Because of this coupling a change in the intensity of one line, for example due to the feedback of that light

into the laser cavity, results in a change in the other, of opposite sense. This enables the infra-red line intensity to be monitored by observing the red line intensity with a photo-multiplier. Using the red light output in this way (ASHBY et al, 1964) limits the overall frequency response of the system to about 3 Mc/sec.

In the actual interferometer M_1 was concave, with a focal length of 1 meter, and M_2 was plane. Both had dielectric coatings chosen so that they would reflect both red and infra-red. M_3 was an aluminised concave mirror, with a focal length of 1 meter, and it was placed 250 cm from M_2. The TEM_{ooq} mode pattern, in the red, was selected, i.e. a single spot. The angular divergence under these conditions was about 1 milliradian.

It was found that the red and infra-red beams did coincide, but were emitted at an angle of about 1 milliradian to each other and the infra-red beam divergence was four times greater than that of the red beam. By including a variable stop between M_2 and M_3 (see Fig.1), it was shown that only that portion of the infra-red beam common to the red was effective in controlling the feedback into the laser cavity.

3. THE DISCHARGE PARAMETERS

The circuit associated with the z-pinch is shown in Fig.2(a). A capacitor bank of 3 μF, at 30 kV, was connected, via a spark gap and a 0.5 Ω damping resistor, to the ends of a 1.5 meter x 8.5 cm internal diameter cylindrical pyrex tube. Six return current straps ran the length of the tube. The maximum current of 20 kA was attained after 2.6 μsec., and the first current zero occurred after 8 μsec. (see Fig.2(b)).

The plasma was observed to constrict to a diameter of 2.5 cm, and after current maximum rapidly expanded to the wall. No instabilities were observed and after the plasma reached the wall no internal structure could be seen, using an image converter camera directed radially.

4. THE EXPERIMENTAL RESULTS

The spatial resolution of the electron density was limited by the diameter of the laser beam, which was 3 mm. The interferometer was first aligned axially, at various radial positions. This arrangement enabled the radial density to be measured during the period 20 - 110 μsec. For earlier times the interferometer was sighted radially, through quartz windows in the pyrex walls. Typical results are shown in Figs.3, 4(a) and 4(b).

The intensity-time variation of the laser light was recorded by an oscilloscope. Adjacent maxima or minima represent the time for the effective path length to change by half a wavelength. This corresponds to an electron density change given by:-

$$\delta n = 2.25 \cdot 10^{13} \lambda \ell \text{ electrons cm}^{-3}$$

where, λ, the probing wavelength, was $3.39 \cdot 10^{-4}$ cm; ℓ, the path length in the plasma, was 148 cm along the axis, and 8.5 cm across a diameter. The change in electron density corresponding to the time interval between minima was $2.25 \cdot 10^{14}$ axially and $3.3 \cdot 10^{15}$ radially.

Fig.3 is an example of an oscilloscope trace with a radial light beam and Fig.4(a) is a trace taken in the axial direction for r = 0. Fig.4(b) is for r = 3 cm. In Fig.3 only the last two cycles can be counted since the first cycle occurs during the pinch phase of the discharge when the electron density is changing more rapidly than can be detected by the interferometer.

In Fig.5 the analysis of the results is presented to show the decay of the electron density as a function of time. Curve 'A' is drawn from the radial data, the 'B' family of curves from the axial data. Each member of the 'B' family is the average of three separate determinations, which were reproducible to within 5%. An interesting feature of the 'B' curves is their convergence to a value of $2.3 \cdot 10^{15}$ electrons cm^{-3} at 20 μsec. This agrees with the value from the 'A' curve at the same time.

Fig.6 illustrates the agreement between several independent measurements of the electron density under the same conditions. The techniques were firstly a determination of the Stark profile of H_β using an oscillating Fabry-Perot interferometer (PEACOCK and HILL, 1964) a similar determination using a spectrometer and rotating mirror camera (PEACOCK, 1964), and thirdly a measurement of the radial electron density with a 2 mm microwave interferometer (NEWTON and NIBLETT, 1964). The scatter of 5% in the results from these different techniques attests the reliability of the laser interferometer measurements. This point will be further discussed later in light of apparently conflicting results due to GERARDO and VERDEYEN, (1963). Further, since the Stark-broadened measurement depends on the ion electric field at one point, whereas the interferometer integrates over the line of sight, Fig.6 is, therefore, strong evidence for the axial uniformity of the plasma. The actual profiles of the electron density, derived from Fig.5, are shown in Fig.7, for various times.

5. DISCUSSION OF THE RESULTS

The agreement between the various techniques is particularly interesting in view of the work by Gerardo and Verdeyan, who used

a similar hemispherical laser cavity, operating at 1.15 μ, with an external mirror. They showed, following the theoretical work of BOYD, GORDON and KOGELNIK (1961, 1962), that transverse modes can be excited in the external cavity of the general form TEM_{mpq}, where m and p are transverse mode indices and q is the axial mode index. A change in q, m or p of 1 causes one cycle in the laser output intensity, as described above. The actual contribution of the transverse modes to the total change depends on the parameter d/R, where d is the length of the external cavity and R is the radius of curvature of the external mirror. The following equation shows the total change:-

$$\delta n = \delta q + \frac{\delta m + \delta p}{\pi} \cos^{-1} \left(1 - \frac{d}{R}\right)^{0.5}$$

δq is the change in the axial mode, i.e. when $R = \infty$ and δm and δp are the changes in the transverse modes.

In the experiments of Gerardo and Verdeyen $d = R/2$, i.e. the minimum density change measurable by changes in m or p is one quarter of that measured by changes in q, they therefore show that interferometer and Stark broadening results agree only if the transverse modes are taken into account. In the present experiment, however, $d = R$ and from the above equation:-

$$\delta n = \delta q + \frac{\delta m + \delta p}{2}$$

and the transverse modes should contribute an extra 50% to the axial change; reference to Fig.6 reveals that this is not so. The probable reason for this is that, as mentioned earlier, only the portion of the infra-red beam common to the red actually contributes to the detected interference signal, so the effect of the transverse infra-red modes would not be included. It is possible that in a laser interferometer operating completely at 3.39 μ the effect of the off-axis modes may be important.

6. ANALYSIS OF THE RESULTS

The three major processes which cause the decay of the free electron density in the afterglow of a hydrogen discharge are ambipolar diffusion, attachment and recombination. The decay rate can be represented by the equation:-

$$\frac{\partial n}{\partial t} = D_a \nabla^2 n - h\nu n_i n - \alpha n^2$$

n is the electron number density, D_a is the ambipolar diffusion coefficient, h is the attachment probability, ν is the frequency of electron collisions with an attaching impurity ion, of density n_i, and α is the recombination coefficient.

To assess the relative importance of the terms of the above equation it is convenient to replace $D_a \nabla^2 n$ by $D_a n/\Lambda^2$, where Λ is the characteristic diffusion length, which, for a plasma contained in a cylinder, length ℓ radius r, is given by BOYD and KOGELNIK (1962):-

$$1/\Lambda^2 = (\pi/\ell)^2 + (2.4/r)^2$$

In the present experiment ℓ was 148 cm and r was 4.25 cm, hence Λ was 1.76 cm.

The values of α, D_a, h and ν have been determined by a number of authors. From CRAGGS and HOPWOOD (1947) and CRAGGS (1963), α was $1.7 \cdot 10^{-11}$ $cm^3 sec^{-1}$. BIONDI and BROWN (1949) gave a value in torr, also they showed that $D_a \propto T_g^2$. The two density regions covered by the curves 'A' and 'B' of Fig.5 are those with n_e between 10^{15} and 10^{16}, and n_e between 10^{14} and 10^{15}. T_e was close to T_g and was measured to be 10^4 °K and p was 0.1 torr, therefore, D_a was 10^5 $cm^2 sec^{-1}$. Finally, bearing in mind that the most important attaching impurity present is usually oxygen, the maximum amount of oxygen present was less than 0.5%, measured spectroscopically

(NEWTON, 1964), therefore the maximum value of $h\nu n_i$ was 50 sec^{-1}, since at a temperature of 10^4 °K, h is $5 \cdot 10^{-5}$ and ν is $10^{10} sec^{-1}$ (BROWN, 1959). ν was $10^{10} sec^{-1}$ (NEWTON, 1964).

The values of the terms of the equation at $n_e = 5 \cdot 10^{15}$ and $5 \cdot 10^{14}$ are given in the accompanying table:-

n_e	$5 \cdot 10^{15}$	$5 \cdot 10^{14}$
αn_e^2	$4.4 \cdot 10^{20}$	$4.4 \cdot 10^{18}$
$D_a n_e / ^2$	$1.6 \cdot 10^{20}$	$1.6 \cdot 10^{19}$
$h\, n_i n_e$	$2.5 \cdot 10^{17}$	$2.5 \cdot 10^{16}$

Thus attachment can be ruled out as a loss mechanism, while recombination is important in the first density range and diffusion in the second.

These findings are borne out by the temporal variation in the electron density within the two ranges, as shown in Figs.5 and 8. Fig.8 is a plot of $1/n_e$ against time, and during the early part of the decay, i.e. 10 - 20 μsec, the graph is linear; in support of the thesis that the predominant loss mechanism was recombination. From the slope of the graph α was $2.2 \cdot 10^{-11} cm^3 sec^{-1}$, which is in good agreement with the value quoted above.

From Fig.5 the characteristic diffusion times can be found as a function of radius, and the value of D_a determined from the equation:-

$$D_a = \Lambda^2/\tau$$

varied from 25 to 18 μsec as r was changed from 0 to 3.5 cm, or D_a varied from 1.2 to $1.7 \cdot 10^5 cm^2 sec^{-1}$. Both values are in agreement with the value of D_a quote above. From Fig.5 it also appears that an ambipolar diffusion process is operative near the walls at

30 μsec and after 60 μsec the decay rate is characteristic of ambipolar diffusion over the whole of the plasma cross-section.

7. CONCLUSIONS

The application of gas laser interferometry to the measurement of the electron density in the after glow of a z-discharge has been described. The technique used has proved simple to apply, and has yielded results in close agreement with other more complicated techniques. In particular the experiment demonstrated the good spatial resolution possible, which enabled the changing radial density profile of the discharge to be followed.

Two types of electron loss mechanisms were identified. In the first 10 μsecs recombination was dominant. In the latter stages ambipolar diffusion was dominant. The radial density distribution was radically different during the two periods.

8. ACKNOWLEDGEMENTS

I should like to thank G.E.S. Harding for practical assistance during the experiment, and H.A.B. Bodin and A.A. Newton for many helpful discussions.

9. REFERENCES

ASHBY, D.E.T.F. and JEPHCOTT, D.F. (1963) Appl. Phys. Letters, 3, 13.

ASHBY, D.E.T.F., JEPHCOTT, D.F., MALEIN, A. and RAYNOR, F.A. (1964) (To be published)

BIONDI, M.A. and BROWN, S.C. (1949) Phys. Rev., 75, 1700.

BOYD, G.D. and GORDON, J.P. (1961) Bell Syst. Tech. J., 40, 489.

BOYD, G.D. and KOGELNIK, H. (1962) Bell Syst. Tech. J., 41, 1347.

BROWN, S.C. (1959) Basic data of plasma physics. New York, Wiley.

CRAGGS, J.D. (1963) Sixth Int. Conf. Ionization Phenomena in Gases, Paris, 1963. Proceedings,

CRAGGS, J.D. and HOPWOOD, W. (1947) Proc. Phys. Soc., 59, 771.

GERARDO, J.B. and VERDEYEN, J.T. (1963) Appl. Phys. Letters, 3, 121.

NEWTON, A.A. (1964) Culham Laboratory. (Private communication)

NEWTON, A.A. and NIBLETT, G.B.F. (1964) Culham Laboratory (Private communication)

PEACOCK, N.J. (1964) Culham Laboratory (Private communication)

PEACOCK, N.J. and HILL, E.T. (1964) Culham Laboratory. (Unpublished information)

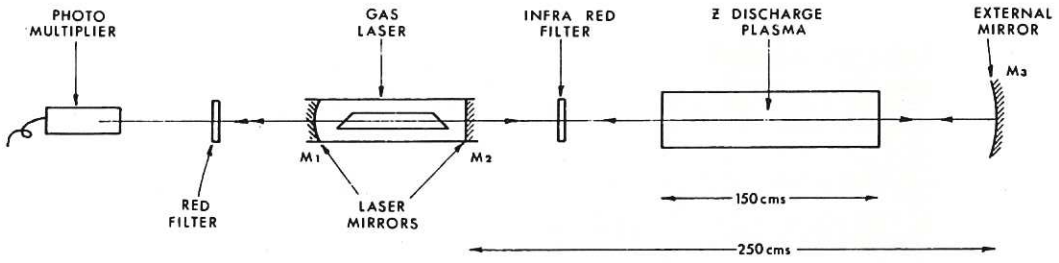

CLM-P60 Fig. 1
Schematic arrangement of the gas laser interferometer

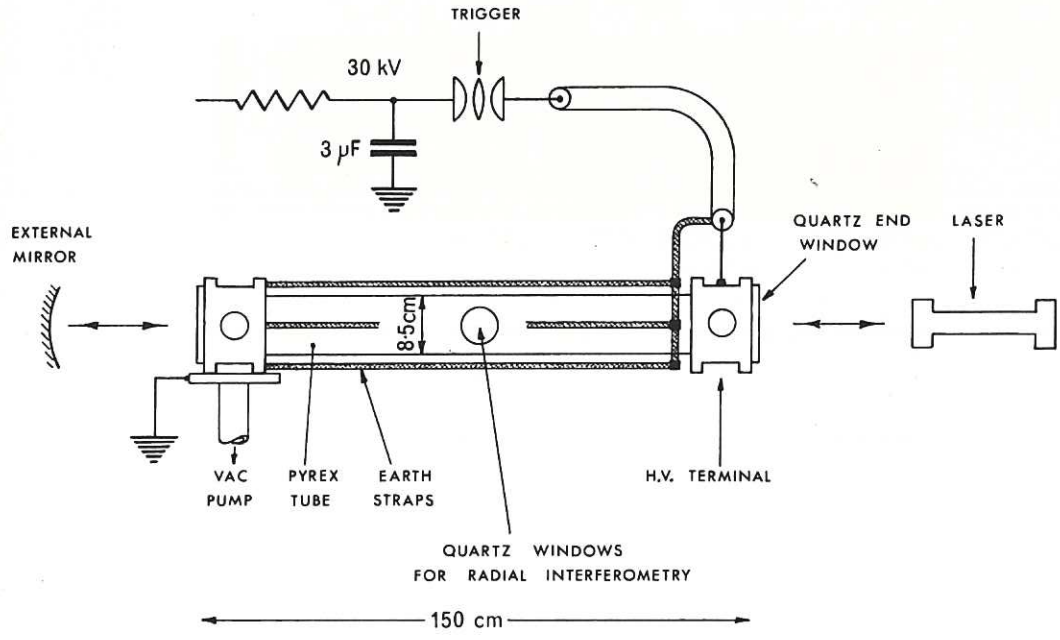

CLM-P60 Fig. 2 (a)
Schematic arrangement of the z pinch discharge

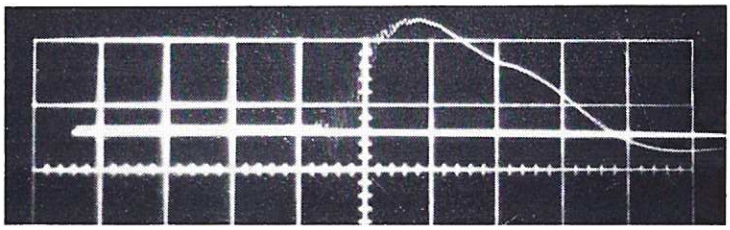

CLM-P60 Fig. 2 (b)
Current waveform (sweep speed 2 μsec/cm)

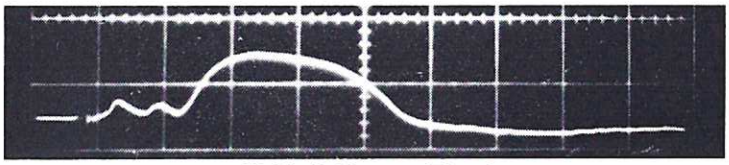

CLM-P60 Fig. 3
Radial interferometer fringes (sweep speed 10 μsec/cm)

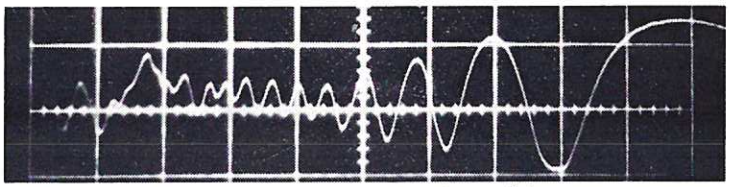

CLM-P60 Fig. 4 (a)
Axial interferometer fringes (sweep speed 10 μsec/cm) on the axis

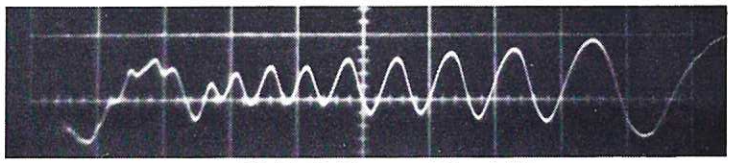

CLM-P60 Fig. 4 (b)
Axial interferometer fringes (sweep speed 10 μsec/cm)
at 3 cm from the axis

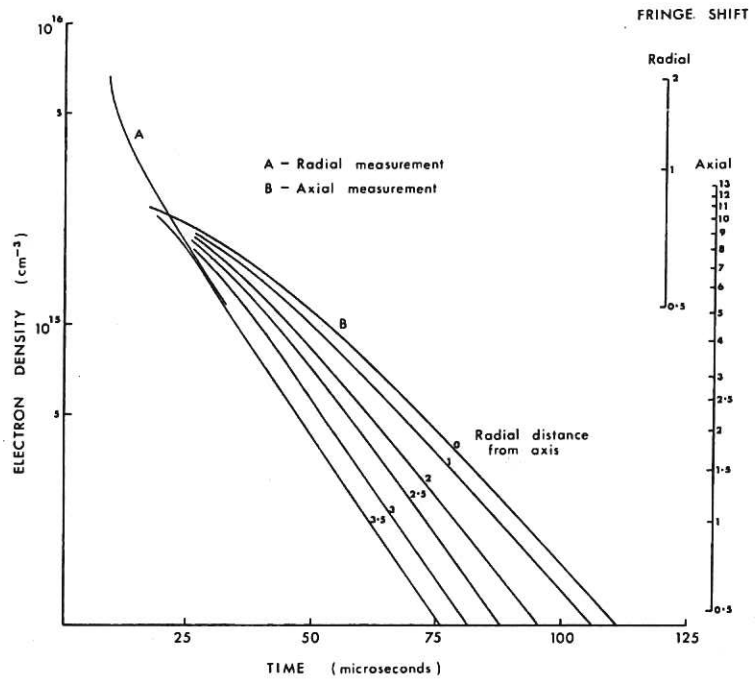

CLM-P60 Fig. 5
Electron density in the afterglow as a function of time and position

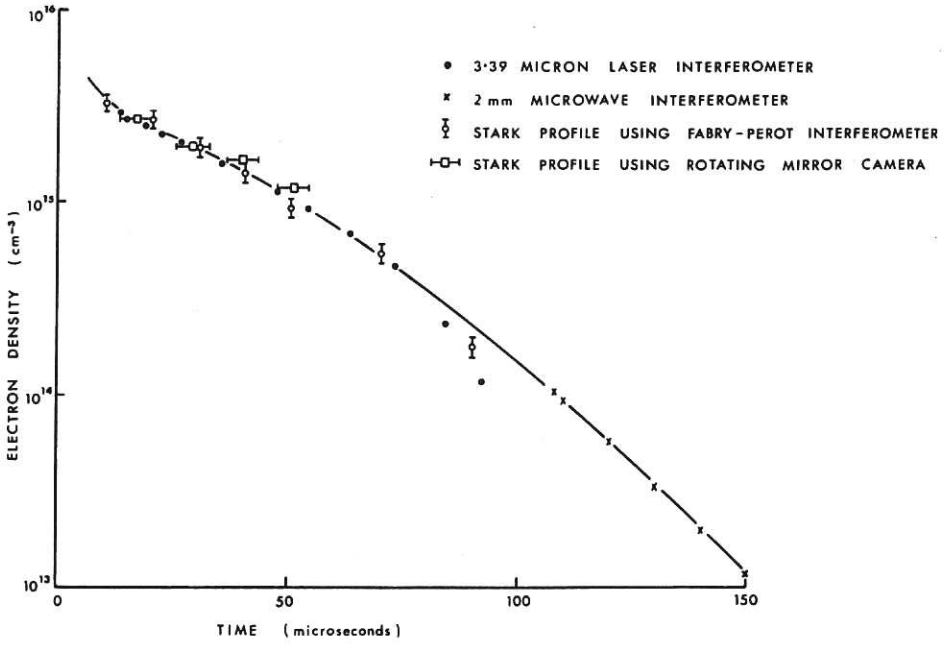

CLM-P60 Fig. 6
Comparison of the results of various electron density determinations

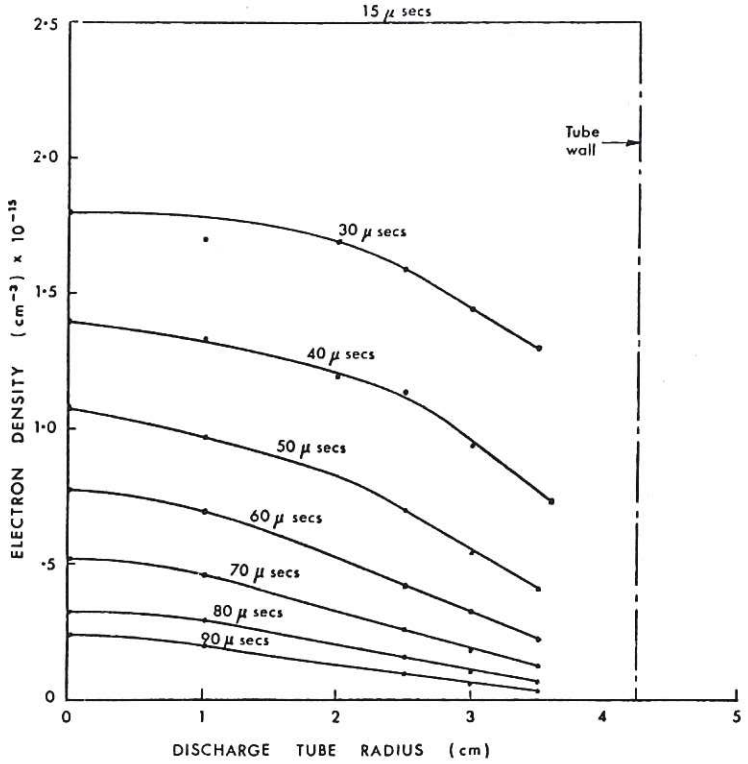

CLM-P60 Fig. 7
Electron density radial profile at various times

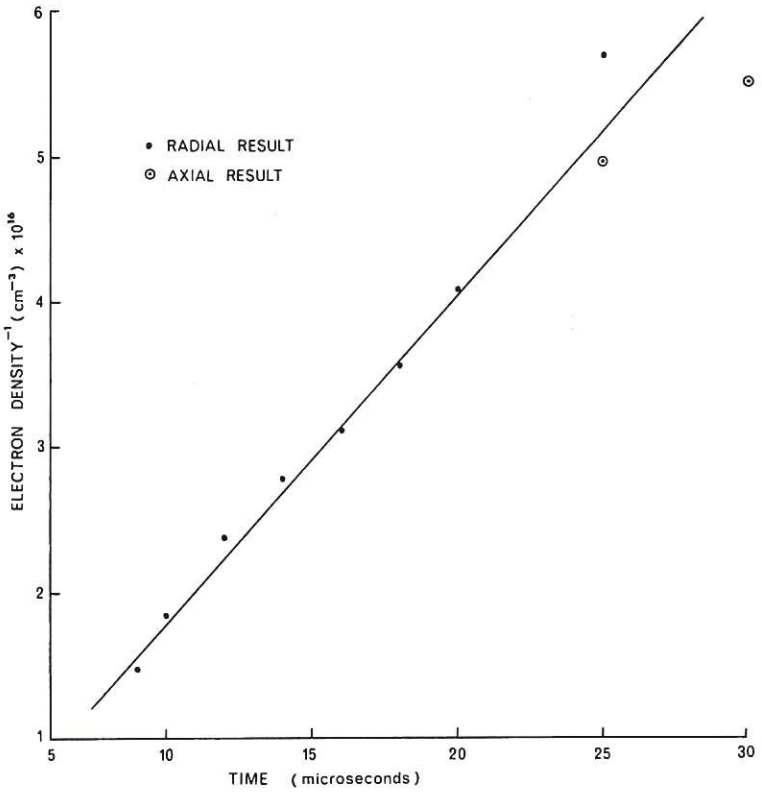

CLM-P60 Fig. 8
Plot of the reciprocal electron density as a function of time in the first 10 μsecs of the afterglow